# A COMPARISON OF TWO FIELD STUDIES OF ACOUSTIC BED VELOCITY: GRAIN SIZE AND INSTRUMENT FREQUENCY EFFECTS

**David Gaeuman, Research Associate, USGS, Columbia Environmental Research Center, Columbia, MO, dgaeuman@usgs.gov ; Colin D. Rennie, Assistant Professor of Civil Engineering, University of Ottawa, Ottawa, ON, Canada.**

## INTRODUCTION

Recent studies (Rennie et al., 2002; Rennie and Villard, 2004) suggest that it may be possible to measure bedload transport rates using measurements obtained with an acoustic Doppler current profiler (ADCP) or similar instrument. The method is based on the ADCP's bottom-tracking capacity, by which relative motion between the ADCP and sediment particles on the stream bed is normally used to detect instrument motion when making water discharge measurements. Rennie et al. (2002) hypothesized that the difference between the apparent instrument trajectory according to bottom-tracking and the actual instrument trajectory is representative of the average velocity of sediment particles on the stream bed. They designated this corrected bottom-track measurement as the bed velocity ($\nu$), and proposed that it can be used to estimate bedload transport rates via an empirical calibration.

Significant obstacles must be overcome before calibrated ADCP bed-velocity measurements can be generally applied for monitoring bedload sediment transport. Perhaps the most obvious difficulty is that physical bedload transport samples can be difficult to obtain under some field conditions, and are themselves often of uncertain accuracy. Thus, precise and reliable transport data with which to calibrate may be unavailable. Secondly, the acoustic response of a given instrument depends to some degree on site characteristics, including the sizes of sediment particles in transport. Bed material sizes can be spatially variable at multiple scales, from within-reach variability associated with element of channel morphology (Lisle et al., 2000) to transitions from gravel to sand at the segment scale (Sambrook Smith and Ferguson, 1995). Bed-material particle size distributions, and hence the sizes of bedload particles in transport, can vary systematically in time at a single location (Rubin and Topping, 2001). The sensitivity of $\nu$ to relatively subtle changes in sediment characteristics typical of sand-bed rivers has not been investigated. Consequently, the extent to which a calibration of $\nu$ obtained at a given site or at a given time can be transferred to similar sites or other times is unknown.

In this paper, we compare bed-velocity responses to bedload transport and flow changes measured with a 1500-kHz Doppler instrument in a sand-bed reach of the Fraser River (Rennie and Villard, 2004) to similar data collected with a 600-kHz instrument in the lower Missouri River. The Missouri River data was collected as part of a project conducted by the USGS Columbia Environmental Research Center (CERC). Our present objective is to explore the adequacy of existing theory for describing differences in bed-velocity responses arising from differences in instrument frequency and reach characteristics. A fundamental understanding of these effects is necessary for assessing the spatial and temporal stability of bed-velocity calibrations, and for the potential development of appropriate corrections to account for varying reach conditions.

## CHARACTERISTICS OF THE STUDY REACHES

All Missouri River data were collected in the navigation channel between 1 and 3 km upstream from the US Interstate 70 bridge in central Missouri. The Missouri River study reach is henceforward referred to as MR. This part of the river contains wing dikes that maintain a deep, narrow navigation channel about 200 m wide between the dike tips. Thalweg depths range between about 7-10 m when the river is near flood stage. The reach-averaged water surface slope is consistently about 0.00016 irrespective of stage, and thalweg depth-averaged flow velocities frequently exceed 2.5 m/s. Bed material is primarily sand, with a median particle size ($D_{50}$) of about 0.0006 m in diameter and a 90$^{th}$ percentile particle size ($D_{90}$) of 0.0022 m. Most of the bed is covered with dunes that are 1-2 m high and between 10 and 60 m in wavelength. The 2-year annual peak discharge is 5,747 $m^3$/s (USACOE, 2003).

Sea Reach (designated SR below) is a sand-bed estuarine distributary of the Fraser River about 300 m wide and less than 5 m deep at low tide when the bed is mobile. Depth-averaged flow velocities are normally less than 1 m/s. $D_{50}$ was found to be about 0.00025 m for all sample locations. A $D_{90}$ of 0.002 m was recorded for 40 of the 68 samples, whereas 0.00035 m was recorded for the remaining 28 samples. The mean annual peak flow of the Fraser River at the Hope gage (155 km upstream) is 8,800 $m^3/s$ (Rennie and Villard, 2004). However, the study reach occupies a distributary arm in which discharge in not accurately known. The reach is tidal in nature, so that stages and water surface slopes lack consistent relationships to discharge. No evidence of salt wedge intrusion or flow reversal was observed during the sampling period.

## METHODS

**Field Methods:** Both data sets compared in this paper consist of hydraulic and bed-velocity measurements recorded with commercially-available acoustic Doppler instruments while simultaneously collecting bedload sediment samples and global positioning system (GPS) data . Rennie and Villard (2004) recorded acoustic data in 2001 with a narrowband Sontek 1500-kHz acoustic Doppler profiler (ADP). Actual instrument velocities were tracked using differential GPS. MR data was obtained in 2004 and 2005 using a broadband RD Instruments 600-kHz Workhorse Rio Grande ADCP and real-time kinematic (RTK) GPS. Aside from the differences inherent in the use of instruments manufactured by different companies, the acoustic data collection procedures were similar. More complete discussions of bottom-tracking, bed velocity, and sources of errors in these measurements are available in Rennie et al. (2002), Rennie and Villard (2004), and Gaeuman and Jacobson (2005).

Bedload sampling was conducted from boats using similar Helley-Smith samplers in both studies. Helley-Smith samplers are pressure-difference samplers with a nozzle expansion ratio of 3.22 and a sampling efficiency of about 100-150% (Edwards and Glysson, 1999). CERC personnel collected 80 Helley-Smith bedload samples from MR during the 2004 field season, and Rennie and Villard (2004) collected 68 samples at their Fraser River site. All sampled transport rates are reported herein as bedload capture rates ($c_B$), defined as the mass of sediment caught in the sampler divided by the sampler residence time on the bed in seconds. Especially at MR, where flow is both deep and turbid, the position of the sampler on the bed with respect to bed topography could not be determined. High spatial variability in the bedload transport rate associated with bedform position (Gomez and Troutman, 1997) undoubtedly contributed to variability in the sampling results. Although sampler position on the bed was known only approximately, spatial averaging inherent in the acoustic measurements ensured that the concurrently-recorded acoustic data encompassed the sampler position. This spatial averaging is the result both of slight boat motions during the sampling period and because ADCP measurements are based on multiple acoustic beams directed radially outward from the instrument. Rennie et al. (2002) and Gaeuman and Jacobson (2005) describe the footprint characteristics of the respective instruments.

Flow conditions at the time of MR data collection were highly variable. Data were collected on a total of 28 different days at discharges ranging from about 1,110 to about 5,380 $m^3/s$. However, only selected subsets of these data are reported in this paper. Paired $\nu$ and Helley-Smith bedload samples were obtained in 2004 only. Although MR bedload samples were collected in 2005 as well, they were obtained using a BL-84 bedload sampler, and so are not directly comparable to the SR samples. A second subset of data was selected for comparing acoustic response characteristics, independent of the availability of Helley-Smith bedload samples. Depth-averaged flow velocities and $\nu$ were generally much larger at MR than at SR. The maximum sampled values of these variables at MR were 2.38 m/s and 0.62 m/s, whereas the corresponding maxima recorded at SR were just 1.06 m/s and 0.18 m/s. In order to compare data collected over a similar range of $\nu$, only the 111 MR samples for which $\nu \leq 0.2$ m/s are included in the following comparisons of bed-velocity response to hydraulic conditions. The complete set of MR data indicates that the nature of the bed-velocity response may change at high transport stages; those data are reported elsewhere (Gaeuman and Jacobson, submitted). All Fraser River samples were collected on 4 consecutive days during the June, 2001 freshet (flood). Discharge through the reach was not measured.

**Data Processing Method:** Bed-velocity magnitudes for each sample location were computed as the square-root of the sum of squared east-west and north-south bed-velocity components. Each directional velocity component was obtained by averaging the results of a large number of acoustic pings collected over several minutes at each location. Time-averaged ADCP data were also used to determine depth-averaged downstream flow velocities ($U$) and flow depths ($h$) at all sampling locations. These measurements were then used to estimate additional hydraulic parameters, including the shear velocity ($u_*$) and shear stresses. To compare shear parameters from the two study locations, it is necessary to select a method for estimating them that will produce reasonable results at both sites. A simple means for estimating $u_*$ is to apply the standard expression, $(ghS)^{0.5}$, where $S$ is slope of the energy grade line, which is typically approximated by the slope of the water surface. This method can be conveniently applied at MR, since repeat surveys indicated that the reach-averaged water surface slope was essentially constant over a wide range of discharges. However, SR is tidal, so that the energy slope changes constantly in response to sea level change. Together with generally low water surface slopes, the dynamic nature of the energy slope made it impractical to estimate the energy slope from the water surface slope. Thus, equations that require $S$ to estimate shear stress or channel roughness cannot be directly applied to SR data. Rennie and Villard (2004) chose to estimate $u_*$ with:

$$\frac{U}{u_*} = 2.5\ln\left(\frac{12h}{3D_{90}}\right) \tag{1}$$

A drawback of this approach is that the results are sensitive to the value chosen for the bed roughness height, which Rennie and Villard (2004) assumed to be equal to $3D_{90}$, This implies that the shape of the vertical velocity gradient is influenced primarily by grain resistance. This assumption may be appropriate for SR, where bedform development was minimal, but not for MR, where large bedforms were observed. Shear velocities used for the present analyses were therefore computed using an alternative method that can be applied to either site with equal validity. First, mean slopes were computed for both reaches using the Lacey formula, as presented by Raudkivi (1998):

$$U = 10.8h^{\frac{2}{3}}S^{\frac{1}{3}} \tag{2}$$

in which $U$ and $h$ were replaced with their mean values for each reach, and the numeric constant was changed to 7.6 so that Equation (2) would yield the mean velocity measured at MR using the known mean slope of 0.00016. This adjustment is justified because the original Lacey analyses incorporate assumptions regarding the scaling of the channel geometry based on measurements of artificial canals in British India (Lacey, 1930). The mean depth for all MR acoustic samples included in this analysis was 7.0 m ($\sigma$, standard deviation, = 1.63 m), and the mean $U$ was 1.51 m/s ($\sigma$ = 0.30 m/s). Inserting the mean values for $h$ (3.7 m, $\sigma$ = 0.46 m) and $U$ (0.69 m/s, $\sigma$ = 0.17 m/s) at SR in Equation (2) using the coefficient calibrated with the MR data (7.6) produced an estimated mean slope for SR of 0.00005. Mean values for $U$, $h$, and $S$ were then inserted into the definition of the Chezy roughness coefficient to yield a mean roughness coefficient for each study site:

$$\overline{C} = \overline{U} \Big/ (\overline{h}\,\overline{S})^{0.5} \tag{3}$$

where bars over the variables indicate mean values. For SR, the mean value of C was estimated to be 48.9. This value of $C$ was used to compute $u_*$ for each sample according to:

$$u_* = Ug^{0.5} \Big/ C \tag{4}$$

Repeating the application of Equations (3) and (4) to the MR data yielded an average Chezy coefficient of 45.2, and an average value of $u_*$ that is nearly identical to the average value estimated from $(ghS)^{0.5}$ (0.1045 vs. 0.1041). Pronounced changes in bedform development noted at different discharges at MR strongly suggest that $C$ is highly variable there, so that values of $u_*$ computed as $(ghS)^{0.5}$ are probably more reliable for that site. Nonetheless, for consistency across sites, we use $u_*$ based on constant $C$ for the analyses presented below. Total boundary shears stresses ($\tau$) for both sites were obtained from $u_*$ using $\tau = \rho u_*^2$, and dimensionless shear stresses ($\tau^*$) were calculated according to $\tau^* = \tau/g(\rho_s - \rho)D_{50}$, where $\rho$ is the density of water and $\rho_s$ is the density of the sediment particles. Some of the total boundary shear stress is expended in form drag associated with bedforms and turbulence in the water column, so only a portion of $\tau^*$ is available for entraining sediments at the bed. We estimated dimensionless shear stress at the bed, or skin friction, with the relation of Wright and Parker (2004).

$$\tau_{sk}^* = 0.05 + 0.7(\tau^* F^{0.7})^{0.8} \tag{5}$$

It is worth noting that a general model for accurately predicting skin friction has yet to be developed (McLean et al., 1999). Models that are reasonably successful for predicting skin friction in laboratory settings may be inadequate for evaluating the conditions found in large sand-bed rivers (Wright and Parker, 2004). Equation (5) was developed specifically for application in these types of environments.

## CONCEPTUAL FRAMEWORK

It is assumed that the magnitude of the bed velocity can be related to the velocity of sediment particles in the bedload layer ($u_b$) by an equation of the form:

$$\nu = B u_b \tag{6}$$

where $B$ is an unspecified function ranging between 0 and 1. Little can be said regarding the form of $B$, except that it is related to both particle entrainment and the strengths of acoustic backscatter from the entrained particles, i.e., $B = f(\tau_{sk}^*, k_s)$, where $k_s$ is the normalized backscattering cross section (Thorne and Hanes, 2002):

$$k_s = \frac{f}{\sqrt{0.5D\rho_s}} \tag{7a}$$

$$f = C_0\left(\frac{1.1(0.5Dk)^2}{1+1.1(0.5Dk)^2}\right) \tag{7b}$$

$$C_0 = 1.1\left\{1-0.25\exp\left[-((0.5Dk-1.4)/0.5)^2\right]\right\}\times\left\{1+0.37\exp\left[-((0.5Dk-2.8)/2.2)^2\right]\right\} \tag{7c}$$

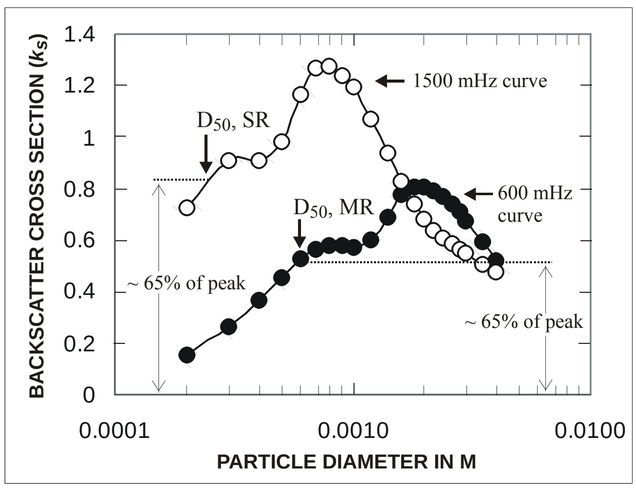


Figure 1 Normalized backscatter cross section as a function of particle diameter. Values of $k_s$ for the median particle size are about 65% of the peak value at both sites.

In Equations (7a), (7b), and (7c), $D$ is the diameter of the entrained particles and $k$ is the acoustic wave number, defined as $k = 2\pi f_i/c$, where $f_i$ is the frequency of the instrument and $c$ is the speed of sound in water. $k_s$ is thus primarily a function of the size of the sediment particles in motion and the acoustic frequency of the instrument being used. Figure 1 compares values of $k_s$ as a function of particle diameter for instrument frequencies of 600 and 1500 kHz. The strength of a backscattered 1500-kHz signal from individual particles reaches a peak for particles less than 1 mm in diameter, whereas the backscatter strength for a 600-kHz signal reaches maximum values for particles larger than about 1.5 mm in diameter. The strength of the total backscatter signal from a population of discrete particles within a sampled volume of water is proportional to the product of $k_s$ and the square root of the mass concentration of the particles (Thorne and Hanes, 2002). In the case of bed-velocity measurements, the relevant backscattering particles are presumed to be moving within the bedload layer or as concentrated suspended sediments moving immediately above the saltating bedload. However, it is also possible for $\nu$ to incorporate backscatter from suspended particle moving 10's of cm above the bed. The significance of this circumstance, which is commonly referred to as water bias (RD Instruments, 1996), will be considered later.

The expected behavior of Equation (6) is summarized as follows. If $\tau_{sk}^*$ is near the threshold for particle entraiment ($\tau_c^*$), the concentration of particles in motion will be low, their total acoustic backscatter strength will be small relative to the backscatter reflected from the immobile bed surface, and $\nu$ will be << $u_b$. If $\tau_{sk}^*$ is increased to a value many times larger than $\tau_c$*, the concentration of moving particles will increase, their total acoustic backscatter strength will increase, and ν will increase. As the cross sectional density of the moving particles approaches 100%, ν will presumably approach $u_b$. Additionally, for a given bedload layer concentration, larger particles will generate stronger acoustic backscatter and larger values of ν.

## HYDRAULIC COMPARISONS

Both MR and the SR data show an approximately linear relationship between $U$ and ν for $U$ greater than a threshold (Figure 2A). The threshold occurs at $U$ ~ 1 m/s for the MR data and $U$ ~ 0.5 m/s for SR. Similar relations emerge when ν is plotted versus $\tau_{sk}$* (Figure 2B). The threshold for $\tau_{sk}$* at which ν goes to zero is also approximately twice as large for the MR data (~ 0.2) as for SR (~ 0.1). The differences in the y-intercepts of the trend lines in both relations are consistent with the conceptual framework described in the previous section, but each of the two relations requires a slightly different explanation.

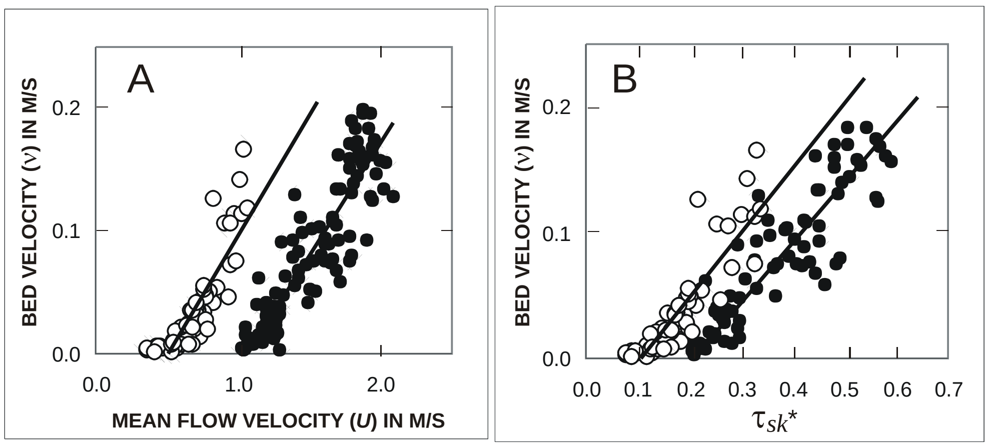


Figure 2 Graphs of A) bed velocity versus depth-average flow velocity and B) bed velocity versus dimensionless skin friction. MR data is shown in black; SR data is shown in white.

For the relation involving $U$ (Figure 2A), the difference in the intercepts is best explained in terms of the difference in bed-material particle sizes in the two study areas. The $D_{50}$ at SR is slightly less than half the $D_{50}$ at MR. As a result, $\tau_c$* at SR is about half that of the Missouri site. As can be seen by numerical experiments with Equations (4) and (5) or careful inspection of their form, $\tau_{sk}$* scales approximately linearly with $U$. A decrease in grain size of 50% therefore translates directly into a corresponding 50% decrease in the threshold $U$ at which ν becomes non-zero. In this case, instrument frequency is a secondary consideration. All that is required is that $k_s$ is sufficiently large for the particle sizes considered and the instrument frequency to generate a measurable signal. It is unclear whether the 600-kHz ADCP would have begun to detect bed motion at SR when $U$ reached 0.5 m/s. If it did, the relative backscatter strength per particle would have been weaker, so that the slope of the line would have presumably been flatter. The virtual equivalent of the slopes shown in Figure 2 are likely coincidental, and may reflect the fortuitous fact that the ratios of $k_s$ for the $D_{50}$ present at each site to the maximum $k_s$ for the instrument frequency are similar for both sites (Figure 1).

The difference in the intercepts for the relation involving $\tau_{sk}$* (Figure 2B) cannot be explained by a change in $\tau_c$* because particles size effects are explicitly included in $\tau_{sk}$*. As a preliminary explanation, it is worth pointing out that the acoustic response may be primarily keyed to a grain-size percentile other than the $D_{50}$. Indeed, Figure 1 indicates that for either site the maximum acoustic sensitivity occurs for grain sizes considerably larger than the $D_{50}$, so that somewhat larger grains exert a disproportionably large effect on the measured ν. In addition, incipient motion of the relevant particle size is unlikely to produce a measurable ν. It seems more reasonable to assume that particle motion must be relatively widespread and persistent, although the required degree of mobilization cannot presently be quantified. In any case, both of these considerations imply that the value of $\tau_{sk}$* corresponding to the appearance of non-zero ν (denoted here as $\tau_\nu$*) is somewhat larger than $\tau_c$*. There is, however, no reason to expect

$\tau_v$* to vary as a function of bed-material particle size. Instead, the difference in $\tau_v$* depicted in Figure 2B is related to the instrument frequency alone. The value of $\tau_v$* is approximately twice as large as $\tau_v$* for SR. When averaged over the relevant range of particle sizes (0.00025-0.0022 m) the ratio of $k_s$ for the 600-kHz instrument to $k_s$ for the 1500-kHz instrument is almost exactly 0.5. Thus, the particles sizes that must be entrained to produce an equivalent acoustic response are twice as large for the 600-kHz instrument; this translates directly to the observed doubling of $\tau_v$*. In other words, $\tau_v$* appears to be directly proportional to $k_s$.

These interpretations suggest a possible approach to adjusting ADCP bed-velocity data to account for differences in bed-material particle sizes and instrument frequencies. As a first step, it is useful to recast ν in the dimensionless form, $\nu/u_b$. As $u_b$ is generally unknown, we substitute $U$ for $u_b$, i.e., $\nu/U$ is assumed to be roughly proportional to $\nu/u_b$ for flow conditions in which $\tau_{sk}$* is significantly greater than $\tau_c$*. The linear relationships shown in Figure 2A suggest that this is a reasonable approximation. The only noticeable departure from linearity in the figure is associated with a small cluster of points indicating locations at SR where ν exceeded 0.1 m/s. All these points correspond to locations where an atypical $D_{90}$ of just 0.00035 was reported for the bed-material. The second step in adjusting the data involves normalizing $\tau_{sk}$* to reflect differences in the signal strengths provided by the two instruments. As noted above, the backscatter signal strength at 1500 kHz is twice a great as at 600 kHz for the same transmit power. A direct comparison between the results from the two instrument can be obtained by comparing values of $K_s(\tau_{sk}*)$, where $K_s$ is the average $k_s$ for the particular instrument over the relevant range of particles sizes. When plotted against $\nu/U$, this adjustment successfully merges the two data sets (Figure 3).

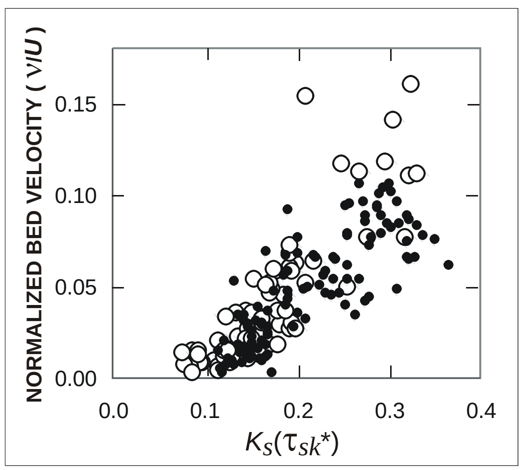


Figure 3 Normalized ν versus normalized $\tau_{sk}$*. MR data is shown in black; SR data is shown in white.

**BEDLOAD TRANSPORT COMPARISON**

Bedload transport rates for all samples obtained at MR were at least an order of magnitude larger than transport rates sampled at SR for given values of ν (Figure 4). This difference overwhelms any possible discrepancies associated with differences in sampler efficiency or other sources of uncertainty. Instead, a large portion of the difference can probably be attributed to differences in the bed-material particle sizes at the two sites. This result suggests that empirical correlations between ν and bedload transport rates may be exceedingly sensitive to subtle changes in the size distribution of the bed-material. As previously noted, the 1500-kHz instrument is approximately twice as sensitive to particles of a given size as the 600-kHz instrument within the range of sizes present at these study sites. For a bed composed of a uniform particle size, it seems reasonable to assume that switching from a 600-kHz instrument to a 1500-kHz instrument would generate an approximate doubling of the ν associated with a given actual sediment transport rate. However, changes in grain size appear to have the potential to exert a much greater effect on the ν-transport relation.

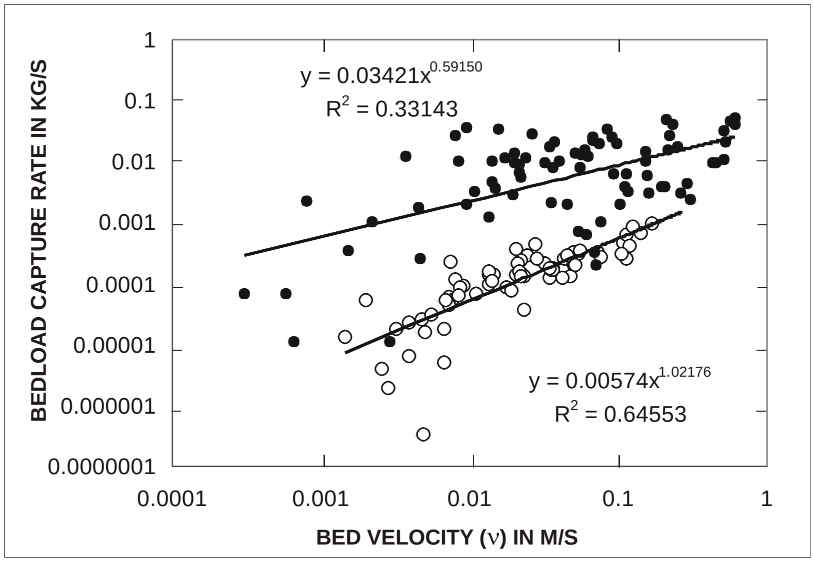


Figure 4 Bedload capture rates versus ν for MR samples (black) and SR samples (white). MR samples are between about 12-20 times larger for the same ν, as estimated from the best-fit power functions for $\nu \geq 0.1$.

Consider a uniformly-graded bed characterized by an arbitrary grain diameter of 0.0005 m and flow conditions given by a dimensionless skin friction based on the bed-material size ($\tau_{sk0.0005}$*) and $U$. If instrument frequency is held constant at 600 kHz and the grain size is doubled to 0.001 m, $k_s$ would increase by approximately 25%. At the same time, assume that a constant dimensionless transport rate is maintained by increasing the skin friction to $2\tau_{sk0.0005}* = \tau_{sk0.001}*$. Because $\tau_{sk0.001}$* has an identical relation to the new stream bed as $\tau_{sk0.0005}$* had to the former bed, the resulting entrainment response should be invariant. There is no reason to suppose that any more or fewer particles would be entrained at any moment in the second situation than in the first. Nonetheless, the particles in transport would be larger by a linear factor of 2, which corresponds to an 8-fold increase in the transported volume. As the acoustic backscatter strength scales with the product of $k_s$ and the square root of particle concentration, simultaneous doubling of the particle and flow scales would therefore produce a 3.5-fold increase in the backscatter strength ($1.25 \times 8^{0.5} = 3.53$). Assuming that ν is approximately proportional to backscatter strength, ν would increase by the same factor. However, the associated increase in the bedload transport rate would equal the concentration increase, i.e., a factor of 8.

We note here that the increase in $\tau_{sk}$ invoked in this thought experiment would be associated with increases in $U$ and $u_b$, which would result in additional increases in both ν and the bedload transport rate. However, these changes would affect ν and the sediment transport rate in a similar manner, and so have no net effect on their ratio. The net result of the particle size doubling is therefore estimated to be an increase in the sediment transport rate associated with the same ν by a factor of about 2.25 (i.e., 8/3.5). Together with the instrument frequency effects incorporated into comparisons between the MR and SR data, bedload transport rates associated with a given ν should be expected to be about 4.5 times greater for the MR data. This accounts for about a third of the difference depicted in Figure 4. Although the remaining difference could plausibly be attributed to bedload sampling error, the possibility of additional acoustic effects cannot be ruled out. A fairly obvious candidate for an acoustic effect that might amplify the magnitude of ν for a given transport rate would be a greater sensitivity to water bias on the part of the 1500-kHz instrument. As is clear from the values of $k_s$ plotted in Figure 1, a 1500-kHz instrument should be considerably more sensitive to the finer particles likely to be suspended high in the water column than is a 600-kHz instrument. The successful collapse of the data shown in Figure 3 was achieved with a simple scaling according to $k_s$ that makes no assumptions regarding where in the water column the backscattering particles are located. This suggests that the cause of the unexplained difference in the relation between ν and $c_B$ lies elsewhere. However, this analysis was limited to consideration of sand-sized particles only, and water bias effects may very well be dominated by the acoustic responses to particles in the silt range where $k_s$ for a 600-kHz signal rapidly converges toward zero. We leave this question unresolved for the time being.

## CONCLUSIONS

The relationship between ADCP bed-velocity measurements and the rate of bedload sediment transport is highly sensitive to changes in the sediment grain size distribution. Because bed-material grain sizes can be variable in both space and time, empirical calibrations for estimating bedload transport rates from $\nu$ cannot be assumed to be stationary, even when confined to a single measurement site. Equations describing backscatter strength as a function of particle size indicate that a two-fold increase in the diameter of sand-size particles will increase the ratio of the bedload transport rate to $\nu$ by a factor of about 2.25. Comparisons between $\nu$ measurements and bedload samples obtained at sites in the Missouri and Fraser Rivers suggest the actual effect of particle size changes on $\nu$ response may be even larger. The threshold dimensionless skin friction below which $\nu$ is zero is approximate twice as large at the Missouri River site than at Sea Reach on the Fraser River. Theoretical considerations suggest that this difference is due to the differences in the operating frequencies of the instruments used at the two sites. However, a similar difference in the threshold mean flow velocities required for non-zero $\nu$ is probably related to differences in bed-material particle sizes between the sites. The data from the two sites can be collapsed to a single relation using normalized versions of $\tau_{sk}$ and $\nu$, in which shear stress is scaled by a frequency- and grain-size-dependent backscattering cross section parameter and $\nu$ is expressed as a fraction of the depth-averaged flow velocity. ADCP bed velocities are derived from a mixture of acoustic backscatter from the moving bedload layer and specular reflections from the immobile bed. The success of the data collapse presented here suggests that this complex acoustic information can nonetheless be interpreted in terms of relatively simple acoustic theory.

## REFERENCES


Edwards, T.E., and Glysson, G.D. (1999), Field Methods for Measurement of Fluvial Sediment, U.S. Geological Survey Techniques of Water Resources Investigations 3-C2.

Gaeuman, D., and Jacobson, R.B. (submitted). “Acoustic bed velocity and bedload dynamics in a large sand-bed river,” Journal of Geophysical Research, doi:101029/2005JF000411.

Gaeuman, D., and Jacobson, R.B. (2005). Aquatic habitat mapping with an acoustic Doppler current profiler: Considerations for data quality, U.S. Geological Survey Open File Report 2005-1163.

Gomez, B., and Troutman, B.M. (1997). “Evaluation of process errors in bed load sampling using a dune model,” Water Resources Research 33(10), pp. 2387-2398.

Lacey, G. 1930. “Stable channels in alluvium,” Proceedings of the Institution of Civil Engineers, London, 229, pp. 259-285.

Lisle, T.E., Nelson, J.M., Pitlick, J., Madej, M.A., and Barkett, B.L. (2000). “Variability of bed mobility in natural, gravel-bed channels and adjustments to sediment load at local and reach scales,” Water Resources Research 36(12), pp. 3743-3755.

McLean, S.R., Wolfe, S.R., and Nelson, J.M. (1999). “Predicting boundary shear stress and sediment transport over bed forms,” Journal of Hydraulic Engineering, ASCE, 125(7), pp. 725-736.

Raudkivi, A.J. (1998). Loose Boundary Hydraulics, A.A. Balkema, Rotterdam.

Rennie, C.D., Millar, R.G., and Church, M.A. (2002). “Measurement of bed load velocity using an acoustic Doppler current profiler,” Journal of Hydraulic Engineering, ASCE, 128(5), pp. 473-483.

Rennie, C.D., and Villard, P.V. (2004). “Site specificity of bedload measurement using an acoustic Doppler current profiler,” Journal of Geophysical Research 109, F03003, doi:10.1029/2003jf000106.

RD Instruments, Inc. (1996). Principles of Operation: A Practical Primer, 2nd Edition for Broadband ADCPs, RD Instruments, Inc., San Diego, CA.

Rubin, D.M., and Topping, D.J. (2001). “Quantifying the relative importance of flow regulation and grain size regulation of suspended sediment transport $\alpha$ and tracking changes in grain size of bed sediment $\beta$,” Water Resources Research 37(1), pp. 133-146.

Sambrook Smith, G.H., and Ferguson, R. I. (1995). “The gravel-sand transition along river channels,” Journal of Sedimentary Research A65(2), pp. 423-430.

Thorne, P.D., and Hanes, D.M. (2002). “A review of acoustic measurement of small-scale sediment processes,” Continental Shelf Research 22(4), pp. 603-632.

USACOE (2003). Upper Mississippi River System Flow Frequency Study, Appendix E: Missouri River Hydrology and Hydraulic Analysis, U.S. Army Corps of Engineers, Kansas City District.

Wright, S., and Parker, G. (2004). “Flow resistance and suspended load in sand-bed rivers: Simplified stratification model,” Journal of Hydraulic Engineering, ASCE, 130(8), pp. 796-805.